Soils and Foundations 2016;56(2):240–250

HOSTED BY

ELSEVIER

CrossMark

The Japanese Geotechnical Society

Soils and Foundations

www.sciencedirect.com
journal homepage: www.elsevier.com/locate/sandf

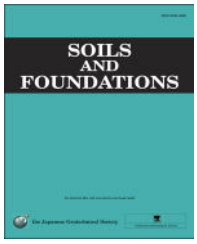

Geotechnical auscultation of a French conventional railway track-bed for maintenance purposes

F. Lamas-Lopez[a,b,*], Y.J. Cui[a], S. Costa D'Aguiar[c], N. Calon[b]

[a]*Ecole des Ponts ParisTech, Laboratoire Navier/CERMES, Marne-la-Vallée, France*
[b]*SNCF, Direction Projet Systèmes, Ingénierie, Département Ligne, Voie et Environnement, La Plaine Saint-Denis, France*
[c]*SNCF, Direction Innovation & Recherche, Paris, France*

Received 24 June 2015; received in revised form 4 November 2015; accepted 17 December 2015
Available online 24 March 2016

Abstract

Prior to renewal or maintenance works on a railway track it is required to perform a proper investigation of the stiffness and thickness of each material constituting the track-bed. In practice, different techniques are used for this purpose. In this study, a comparison of two methods of determining the stiffness of track-bed materials (dynamic penetration and dynamic plate load) is made for a representative French conventional railway line, aiming at optimising the use of different geotechnical auscultation techniques for the railway applications. Firstly, results from geo-endoscopic tests are analysed to define the thickness and nature of the different materials found in the track. Then, dynamic penetration tests (PANDA tests) are performed to evaluate the stiffness of the different layers. Statistical distribution of soil stiffness is analysed for each layer. In addition, the elastic moduli of different materials are estimated from their stiffness using empirical equations. Secondly, dynamic plate load tests using a light weight deflectometer device (LWD) are carried out on surfaces (on tracks and service paths) in order to estimate the dynamic and static moduli of ballast and subgrade. A statistical analysis of the obtained results shows a low dispersion rate and a satisfactory repeatability. The static moduli estimated from LWD tests are found to be consistent with the elastic modulus estimated from PANDA tests, showing that different auscultation methods give complementary information about the mechanical properties of the materials constituting the conventional tracks.

Keywords: Conventional track; Geo-endoscopic test; Dynamic penetration test; Light-weight deflectometer; Statistical analysis; Modulus

1. Introduction

Railway tracks need regular maintenance or renewal, and the corresponding economic issue is in general of great importance. This is particularly the case for the conventional network (Cui et al., 2014). For instance, in France conventional tracks represent 94% of the whole railway network (Duong et al., 2014), and more than 2 billion Euros are spent each year in maintenance operations for these tracks. This situation is related to their history – most of them being constructed at the end of XIXth or the beginning of XXth century. Till the 1970s, the ballast used still did not follow any standards as we know today and was set directly on the subgrade soil (Trinh et al., 2012). As a result, a heterogeneous layer of coarse soil mixed with subgrade soil was formed over time, namely Interlayer (ITL) (Duong et al., 2013), mainly by interpenetration of ballast grains and subgrade soils. The spatial variability of the mechanical properties of ITL and other constitutive materials of railway track-bed as well as its

*Corresponding author at: Ecole des Ponts ParisTech, Laboratoire Navier/CERMES, Marne-la-Vallée, France.
E-mail address: lamas1987@gmail.com (F. Lamas-Lopez).
Peer review under responsibility of The Japanese Geotechnical Society.

http://dx.doi.org/10.1016/j.sandf.2016.02.007

influence on the track degradation were reported by several authors (Alves Fernandes et al., 2014; Dahlberg, 2010; Popescu et al., 2005; Rhayma et al., 2011; Steenbergen, 2013). Thus, there is a need to define a prospection method to determine the mechanical properties of these constitutive materials of track-bed (Connolly et al., 2013; Paixão et al., 2014). Obviously, this kind of information from mechanical prospection can help optimise the renewal or maintenance operations.

Different methods have been used in railway auscultations. They can be divided into geophysical and geotechnical categories. The commonly used geophysical techniques are the multichannel analysis of surface waves (MASW), the ground penetrating radar or down-hole tests. MASW is used to analyse the propagation wave velocities in soil and the thicknesses of different layers of soil (Araujo, 2010; Degrande and Schillemans, 2001). Ground penetrating radar (GPR) defines the thicknesses of different layers of substructure (Su et al., 2011, 2010; Sussmann et al., 2003; Vorster and Gräbe, 2013). The down-hole seismic test is suitable for estimating the shear wave velocities of different track-bed materials (Hunter et al., 2002). On the other hand, most of the geophysical methods present some difficulties in track-bed investigations. For instance, the MASW is not easy to apply on the track surface with ballast because common geophone pins cannot be installed into large grains as ballast due to contact failure (Jacqueline, 2014). Other geophysical methods, as GPR, are more suitable for the qualitative auscultation of track-bed layers and for estimating the thicknesses of track layers.

Among the geotechnical techniques, the most commonly used ones are the dynamic penetration test (as PANDA tests) (Benz, 2009) and the dynamic plate loading test (as the light weight deflectometer, LWD) (Staatsministerium, 2012; Shafiee et al., 2011; Tompai, 2008; Woodward et al., 2014). These tests can help define the quality of a track-bed and the required thickness for different layers. The LWD test estimates the dynamic modulus of a soil, and at each construction stage of a track-bed it help the quality control. The PANDA dynamic penetration test has become a common technique in France (Alves Fernandes et al., 2014) since it allows prospecting the stiffness of existing tracks. The PANDA test measures the tip resistance of different materials. The elastic modulus of materials can be further estimated from their tip resistances using empirical equations (Amini, 2003; Cassan, 1988; Chai and Roslie, 1998; Chua, 1988; Lunne et al., 1997).

Even though different techniques have been successfully employed in railway applications, to the authors' knowledge, there is still no correlation in literature between the elastic modulus obtained from LWD and the modulus estimated from PANDA for ballast (track surface) and subgrade (service path). When the values of modulus of ballast and subgrade are estimated, they can be used to further assess the coherence of modulus estimations for the embedded materials as the ITL, not accessible for the LWD. Thus, a combined analysis using both geotechnical auscultation methods is necessary for a proper investigation of a railway site.

In this study, a conventional track investigation was conducted. A representative site was selected among the 30,000 km French conventional lines for this purpose. Three different geotechnical prospecting methods were used: Geo-endoscopic tests, PANDA tests and LWD. The results were analysed in terms of moduli of different constitutive materials.

2. Experimentation site

A representative experimentation site in a conventional line was required to study the impact of train speed on the behaviour of track-bed materials. Different criteria were imposed to the selection. For instance, track components as rail and sleepers should not have more than 10 years since their last renewal. In addition, the maximum service speed should be comprised between 200 and 220 km/h. A site with tracks in an alignment was also required to obtain the same solicitation at each side of each track. Only 3 sites in France satisfied the imposed criteria: Vierzon, Angouleme and Strasbourg. The site in Vierzon, near Kilometric Point (KP) 187+165 of the 590000 line (from Orléans to Montauban) was finally chosen. This site is located in a zone of cutting of 2 m; it has an UIC class 4 and is composed of two tracks: track 1 going from Orléans to Montauban and vice versa for track 2. Prior to the installation of the sensors, a site investigation was performed. The tests were carried out along 30 m, using as reference the catenary post at KP 187+165. Six auscultation points were defined (see Fig. 1). The geo-endoscopic, PANDA and dynamic loading plate tests performed can be identified in this figure.

3. Prospection methods

3.1. Light dynamic penetrometer PANDA

Like other dynamic cone penetrometers (DCP), the key concept of a PANDA test is to drive a cone (of 2, 4 or 10 cm^2) fixed at the end of a set of rods into the soil using a hammer. Its originality relies in the use variable energy after each hit of hammer, which is measured in an indirect way from the sensors of PANDA. For each hammer hit, the depth of rod insertion and the tip dynamic resistance q_d are recorded automatically. This dynamic tip resistance is obtained from Eq. (1):

$$q_d = \frac{MgH}{(1+a)}\frac{1}{e} \quad (1)$$

where M the hammer mass, H its falling height, a the ratio of masses ($a=P/M$, the rod-system penetrated mass, P, over the hammer mass, M), g the gravity ($g=9.8$ m/s^2), and e the penetration of the rod after impact.

The propagation of a mechanic wave through an elastic material, as the rod, is done through energy transfer. The total energy transported by a wave is divided into two parts (Fairhurst, 1961): kinetic energy $E_K(x,t)$ and potential energy of deformation $E_U(x,t)$. The total energy transferred by the rod

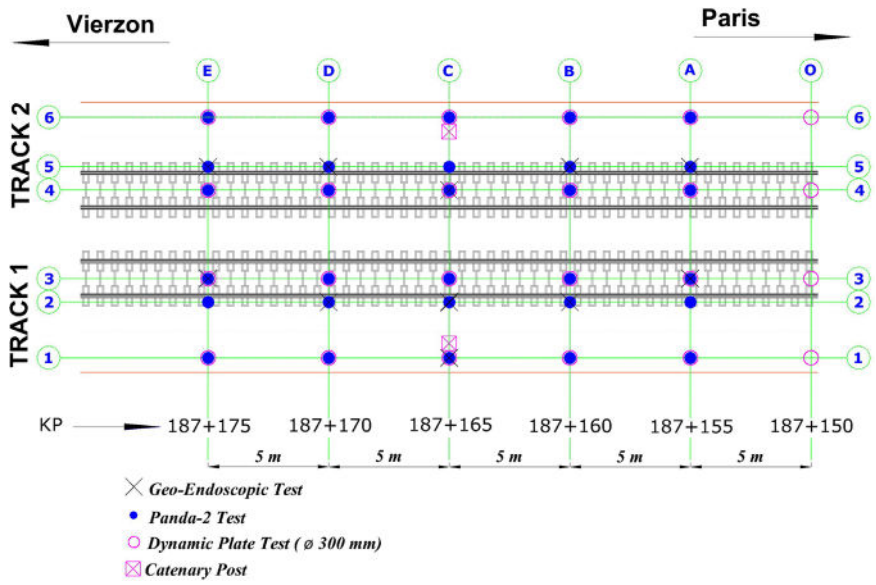

Fig. 1. Prospection tests performed on the 'Vierzon experimental site'.

is determined from the deformation of the rod and the speed of the wave that is estimated from the responses of strain gages and an accelerometer installed at the top of the rod. This method is named EFV and was introduced by Sy and Campanella (1991) to estimate the amount of energy transferred to the rod in the SPT test after each blow. As a variable energy impact is applied, the hammer mass may not influence the measurements (Zhou, 1997). The sensors installed allow the kinetic energy transferred under each blow to be estimated. Another displacement sensor, an LVDT installed at the data logger and connected to the rod, measures the penetration of the rod after each impact. The data logger receives this data after each hit and estimates q_d for each depth.

The advantages of the PANDA penetrometer are not only its weight and size but also its power of penetration, which is sufficient to prospect a large range of different soils: it is able to prospect up to 6 m depth depending on the soil resistance ($q_d < 50$ MPa) and the rod-soil friction. Normally the feasibility of this test depends on the maximum size of particles (50 mm max), but some experiences related to the control of the layer of ballast (up to 60 mm diameter) using PANDA showed valid results (Alves Fernandes et al., 2014; Benz, 2009; Elaskar, 2006; Révol, 2005). Note that to ensure the validity of Eq. (1), the energy impact should be adapted each time in order to obtain a penetration between 2 and 20 mm per impact (Chaigneau, 2001). This makes PANDA test measurements almost continuous (in track-bed scale) and efficient to identify layer thickness or soil compaction defects through the q_d values.

Several authors developed formulas to relate soil elastic modulus to q_d determined from DCP tests (Amini, 2003; Cassan, 1988; Chai and Roslie, 1998; Chua, 1988; Lunne et al., 1997). In this study, the following equations are used to calculate the elastic modulus from PANDA tests. Eq. (2) (Chai and Roslie, 1998) was developed for coarse grain soils. It is also suitable for coarse soils mixed with sand. This equation is used in this study to estimate fresh and fouled ballast modulus.

$$E = 17.6 \cdot q_d^{0.64} \quad (2)$$

Eq. (3) proposed by Chua (1988) was adapted to estimate the elastic modulus of granular soils like sand mixed with other finer soils like clay or silt. It is used here to calculate the moduli of ITL and TL soils.

$$E = 23.2 \cdot \log(q_d) + 12.5 \quad (3)$$

Eqs. (4) and (5) (Lunne et al., 1997) were developed for natural sandy soils.

$$E = 2 \cdot q_d + 20 \text{ if } \forall 10 < q_d < 50 \quad (4)$$

$$E = 4 \cdot q_d \text{ if } \forall q_d \leq 10 \quad (5)$$

3.2. Geo-endoscopic test

The geo-endoscopic test uses a little video camera (wired to a data logger with a soft cable) to observe the soil. The camera is introduced into the hole of a previously performed PANDA test (15 mm of diameter). The results allow a qualitative characterisation of soil, and even the estimation of the soil grain size distribution (Breul, 1995; Haddani, 2005; Haddani et al., 2011).

To perform a geo-endoscopic test, the following materials are required: hollow metric rods (inner diameter of 10 mm), a wired and waterproof little video-camera (with light) and a data logger able to record the camera images and the auscultation depth. Firstly, a 15 mm diameter hole is needed to perform the test. As mentioned before, the hole from a previous PANDA test (same rod diameters) could be used for this purpose. Once the hole is created, the rod is introduced; a wire connected to the camera (IP 65, 8.6 mm of diameter) is descended through the rod from the surface. The hollow rod has a lateral opened window of 5 mm width for taking soil images. To reach deeper auscultation points, additional rods can be added by screwing. A maximum auscultation depth of 6 m can be reached. While the wire is descended at a speed of

5 mm/s, images are recorded by the data logger. The intensity of the light coupled with the camera and the camera focus are controlled from the ground surface. An image is taken every 10 mm of depth and a continuous video is recorded for each test. The images and video obtained from this test allow the determination of different materials constituting the investigated soil layers: the thickness, the soil nature and even whether the soil is saturated or not (water table is spotted using endoscopic cameras). This information can help better analyse the PANDA test results. Consequently, PANDA and geo-endoscopic tests are often coupled for a same auscultation point.

3.3. Light weight deflectometer (LWD)

The dynamic plate loading test using LWD was developed as a technique to determine the dynamic deformation modulus E_{vd} (Staatsministerium, 2012) and the static modulus E_{v2} of soil. This test can be used for soil compaction control and for the determination of the load-bearing capacity of an embankment. The LWD test is faster and easier to operate than the PANDA test.

This test applies a pulse load on soil via a disk-shaped steel plate that is assumed to be rigid. The loading system consists of a 10 kg drop weight that, once released, falls along a rod from 72 cm height until the base disk. The force applied is 7.07 kN on a 30 cm diameter disk. The influenced soil thickness (testing depth) is considered to be equal to the disk diameter. The loading device is positioned on a sphere in the middle of the disk so that only compressive force can be transmitted to the loading plate. An accelerometer is installed in the middle of the plate, recording the maximum vertical displacement of the plate during the impact. The applied stress is assumed to be constant. This test can be conducted on coarse-grained soils and mixed-grains soils as well as fine-grained soils. The percentage of grains in the soil larger than 63 mm must be limited. To obtain a valid measurement on a point, three impacts need to be applied as previous compaction. Then, three new impacts are applied and the mean displacement value by the three impacts is considered. The Boussinesq formula is used to estimate E_{vd}:

$$E_{vd} = \frac{c \cdot (1-\upsilon^2) \cdot \Delta\sigma \cdot r}{\Delta e} \quad (6)$$

where r is the half-diameter of the plate (15 cm), c is the plate coefficient ($c=\pi/2$ if rigid and $c=2$ if soft), $\Delta\sigma$ is the maximum stress applied (considered as constant, 0.1 MPa), υ is the the Poisson's coefficient (0.3) and Δe is the maximum displacement obtained during the test. With the values considered, Eq. (6) can be rewritten as Eq. (7) (Staatsministerium, 2012):

$$E_{vd} = \frac{22.5}{\Delta e} \quad (7)$$

The relationship between the static (E_{v2}) and the dynamic modulus (E_{vd}) is given by Eq. (8) (Livneh and Goldberg, 2001):

$$E_{v2} = 600 \cdot \ln\left(\frac{300}{300-E_{vd}}\right) \quad (8)$$

Note that the LWD test presents some limitations as the auscultation depth of 30–40 cm, range of static modulus comprised between 20 and 180 MPa and a maximum displacement of plate between 0.1 and 2 mm (Staatsministerium, 2012).

4. Test results and discussions

For each auscultation position in Fig. 1, a PANDA test was performed first. Ten PANDA tests was performed on each track and 5 PANDA tests were performed on each service path of the considered section. Then, for some positions (12 in total, see Fig. 1), geo-endoscopic tests were performed using the same hole created during PANDA tests. The geo-endoscopic tests were performed mainly on the track. The prospection on the lateral paths would not be as useful as on tracks because the soil in lateral paths is supposed to be the same as the track's subgrade. Finally, LWD tests were performed on the track centre and lateral paths at every point shown in Fig. 1.

The geo-endoscopic test results were analysed first to identify different materials in track. Fig. 2 shows the geo-endoscopic test images from 4 tests, two tests on each track. Different materials were identified along with their thicknesses by examining the soil grain size, the porosity and colour. The shallowest part of the track is composed of a fresh ballast layer with ballast grains without fouling fines. About 45 cm fresh ballast was found from the tests (Table 1). Deeper in track, a fouled ballast layer was found. The ballast grains are gradually fouled by small grains of about 2 mm, but it seems that there are enough voids to allow rain water move through easily (that is one of the main ballast functions). Fouled ballast thickness was found to be 9 cm in average for both tracks. At deeper levels, a coarse-grained soil without visible voids was identified; this layer is the Interlayer (ITL). The coarse soil content was found gradually different when comparing its beginning and its end. Grains larger than 5 mm diameter are always visible in the ITL soil. One key characteristic of the ITL is that all the coarse grains are totally coated by a fine soil from subgrade (SBG) and from the attrition of ballast grains. On the whole, the ITL soil could be considered as a homogeneous layer in its nature and composition. The different fine soils (less dark, yellow coloured) and the gradually disappearance of coarse grains mark the end of the ITL and the beginning of a Transition Layer (TL). In this first analysis, the beginning of TL is considered when more than 50% of the soil in an image is composed of fine soil from SBG and when the content of coarse grains (larger than 10 mm diameter) starts to decrease from that of the ITL. About 35 cm of ITL was found in each track, but the standard deviation for track 1 (6 cm) is higher than for track 2 (3 cm). Below ITL, the content of coarse grains rapidly attenuates. The fine soil in TL consists of the material of blackish colour from ITL and that of yellowish colour from SBG. The thickness of the TL is an average of 21 cm for track 1 and 23 cm for track 2. Finally, the SBG soil was found below the transition soil. It is quite easy to distinguish the SBG soil as it is composed of fine soil ($d < 1$ mm) of the same nature with very low quantity of

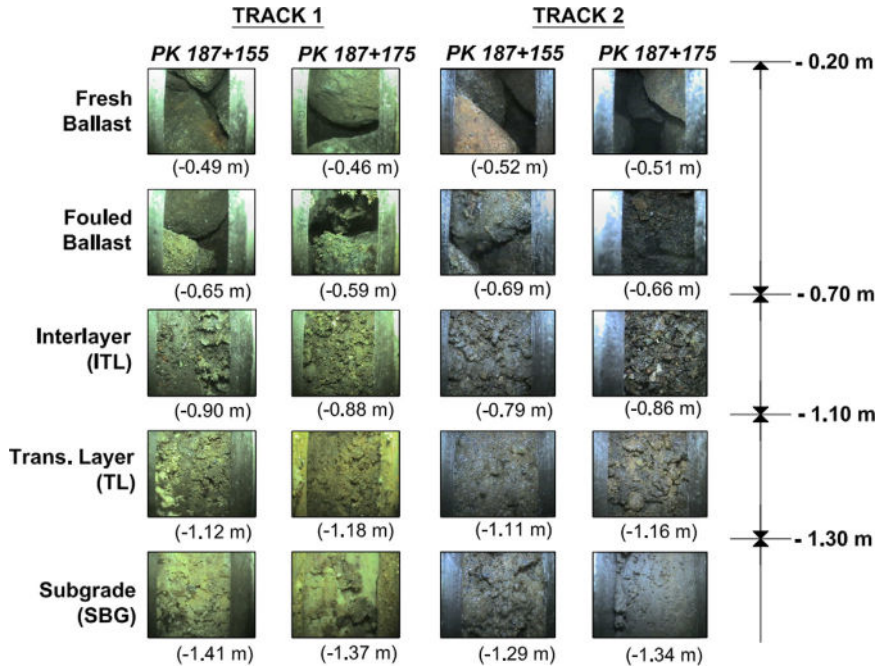

Fig. 2. Different materials observed by geo-endoscopic tests.

Table 1
Thicknesses of track layers from the geo-endoscopic tests performed on tracks 1 and 2.

Track 1 (Thickness of each layer in m)

KP	187+155	187+160	187+165	187+170	187+175	μ	σ
Rail	0.2	0.2	0.2	0.2	0.2	0.2	0.00
Fresh ballast	0.44	0.41	0.45	0.48	0.45	0.45	0.03
Fouled ballast	0.05	0.13	0.08	0.11	0.07	0.09	0.03
Interlayer	0.4	0.38	0.31	0.44	0.34	0.37	0.06
Transition layer	0.25	0.15	0.22	0.21	0.25	0.21	0.04

Track 2 (Thickness of each layer in m)

KP	187+155	187+160	187+165	187+170	187+175	μ	σ
Rail	0.2	0.2	0.2	0.2	0.2	0.2	0.00
Fresh ballast	0.43	0.48	0.42	0.44	0.44	0.44	0.02
Fouled ballast	0.06	0.07	0.11	0.07	0.12	0.09	0.03
Interlayer	0.37	0.35	0.39	0.33	0.31	0.35	0.03
Transition layer	0.23	0.203	0.21	0.24	0.25	0.23	0.02

coarse grains. A first track-bed material composition was then determined for this site: 50 cm ballast (fresh and fouled), 40 cm ITL, about 20 cm TL overlying the SBG.

After analysing the geo-endoscopic tests, the PANDA test results can be analysed. The PANDA tests were stopped when the tip resistance was stabilized at 1.5 m depth under the rail surface (tests on track) and at 1 m depth for the tests performed on the lateral service paths. A typical PANDA tip resistance profile for one on-track test is shown in Fig. 3. It may be noted that the tip average resistance provides different values depending on the material encountered. Four different parts are easily distinguishable: the shallow part corresponds to the ballast layer with low tip resistance values but with an increasing average value over depth as well as a large data dispersion around the average. The low resistance values at surface are due to the ballast grains arrangement when the rod advances. This grain arrangement allows the small penetrometer tip (compared to the ballast grain size) to penetrate easily into the first centimetres of ballast layer. While the tip goes deeper in the track, the grains arrangement becomes more difficult; as a result, the average resistance increases. The data scatter is related to the arrangement of large ballast grains, depending on the contact between the tip and the involved grain. To some extent, this scatter is also due to the size differences between the ballast and rod tip, resulting in tip

resistance values heterogeneity for a coarse-grained soil. The second material in ITL shows a more stable average value of about 90 MPa, but the tip resistances scattered around its average remains significant. Note that this very dense and resistant material has a key role in the mechanical behaviour of a conventional track. The data scatter is also caused by the large grains in the soil. Again, this is an indicator of the heterogeneity of this soil related to the tip size. The TL is characterized by a decreasing average resistance (from 80 MPa to 20 MPa in 20 cm) and a decreasing data scatter. The SBG presents the lowest tip resistance of 15 MPa in average. The data scatter is very limited, showing the homogeneity of the soil. On the whole, there is a good agreement between the thicknesses identified from geo-endoscopic tests and from PANDA tests (Fig. 3).

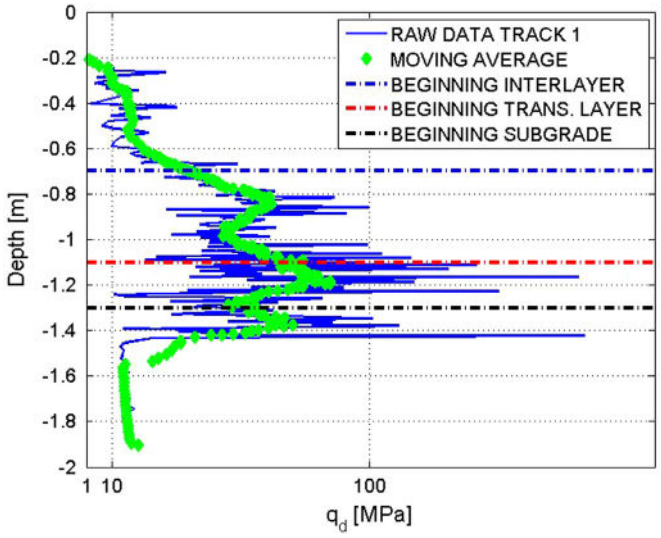

Fig. 3. PANDA test result on track 1 and moving average (Window Length = 8).

When the results from all the 30 PANDA tests (Fig. 1) are analysed by accounting for the thicknesses identified by geo-endoscopic tests, the histogram of tip resistance for Track 1 (Fig. 4) and Track 2 (Fig. 5) are obtained. The relative frequencies of tip resistance are presented for (a) ballast, (b) ITL, (c) TL and (d) SBG. As seen before from a typical resistance on-track profile (Fig. 3), the most frequent resistances of ballast and SBG are lower than those of ITL and TL. There is more scatter of relative frequencies for ITL and TL soils. Moreover, the SBG stiffness scatter is lower and the resistance values are concentrated in the 0–30 MPa range. In both Figs. 4 and 5 the probability density function (pdf) assuming a log-normal distribution is plotted on the histogram as well as the needed parameters to represent the function (average and standard deviation). Comparing the materials in tracks 1 (Fig. 4) and 2 (Fig. 5), it appears that the main difference remains in the TL material. The stiffness of TL in track 1 is higher than in track 2. This is an expected result given that the 20 cm of considered transition depends on the prospection points where PANDA tests were performed. Thus, the TL may present more data scatter and larger difference than ITL and SBG.

Assuming a log-normal distribution of the PANDA resistance, the cumulative distribution frequency (cdf) of each material can be calculated for both tracks (Fig. 6). The resistance distributions show identical results between the two tracks for ballast, ITL and SBG but not for TL where more scatter is observed in the measurements. The log-normal distribution parameters for the tip resistance of each material are presented in Table 2.

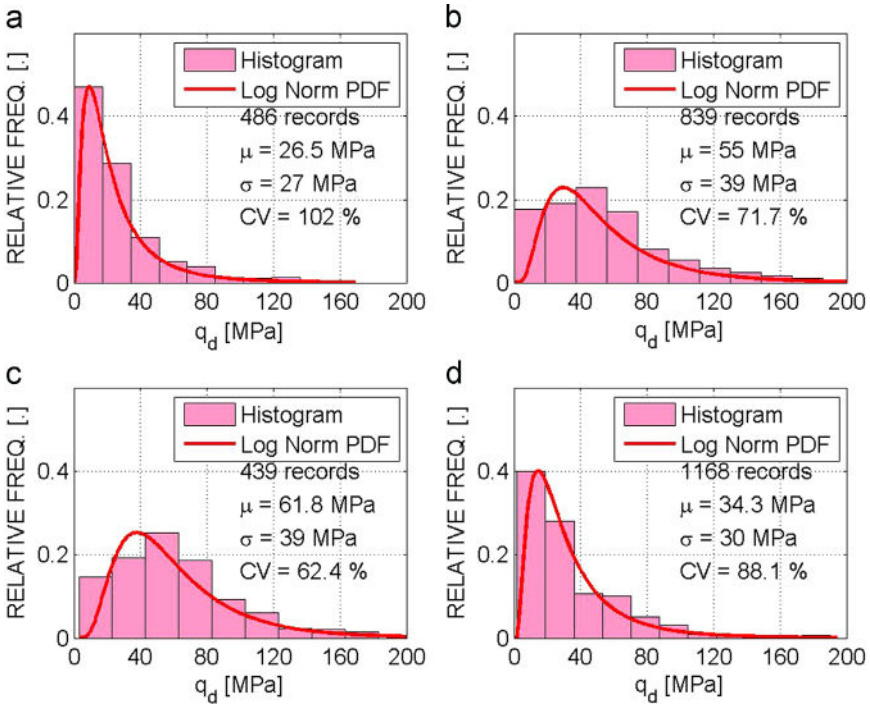

Fig. 4. Histograms of q_d values at (a) Ballast, (b) ITL, (c) TL and (d) SBG for Track 1.

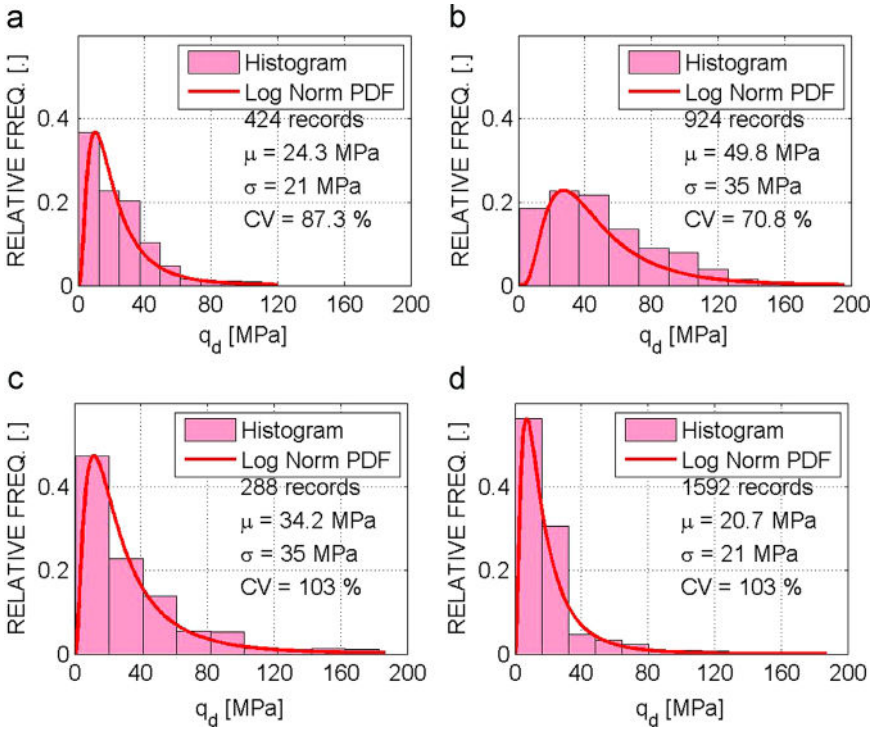

Fig. 5. Histograms of q_d values at (a) Ballast, (b) ITL, (c) TL and (d) SBG for Track 2.

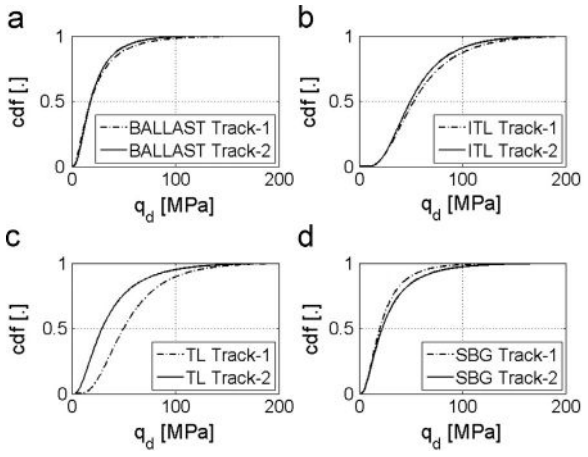

Fig. 6. Log-Normal distribution CDF (cumulative distribution function) for PANDA values at (a) Ballast, (b) ITL, (c) TL and (d) SBG for tracks 1 and 2.

Table 2
Log-Normal distribution parameters of q_d (average and standard deviation) for Ballast, ITL, TL and SBG (PANDA tests performed over tracks 1 and 2).

		Ballast	Interlayer (ITL)	Tran. layer (TL)	Subgrade (SBG)
Track 1	μq_d [MPa]	26.5	55	61.8	34.3
	σ	27	39.11	39	30
Track 2	μq_d [MPa]	24.35	49.8	34.2	20.7
	σ	21.18	35	35	21
T1 and T2	μq_d [MPa]	25.49	60.01	50.61	28.76
	σ	24.43	35.98	37.64	26.41

The PANDA tip resistance results were also used to estimate the soil elastic modulus. Different empirical equations were used depending on the material. As mentioned before, Eq. (2) was applied to the ballast layer, Eq. (3) to ITL and TL materials, and Eqs. (4) and (5) to SBG materials. As a similarity between materials in both tracks was identified with the statistical distributions (except for the TL), the elastic modulus was estimated by taking the tip resistance values for both tracks into account. The average elastic modulus and its standard deviation obtained using the empirical equations are presented in Table 3 for each material. The mean modulus values vary from 127 MPa for ballast to 77.5 MPa for SBG soil. The largest scatter around the average for ballast is consistent with the heterogeneous nature of the ballast. Furthermore, the mean values of the modulus of ITL and TL are halfway from the ballast and SBG results, being 103 MPa for ITL and 95 MPa for TL. Normally, the modulus depends on several parameters such as grain size distribution, stress level, water content, the degree of compaction and the deformation level. The obtained results show that the effect of coarse grain fraction on the modulus is predominant, since the coarse grain fraction decreases with depth from ballast to subgrade. Since ITL soil has coarser grains than TL soil, the estimated elastic modulus for ITL is higher than that for TL.

In order to verify the coherence and validity of the estimations performed using PANDA results, LWD tests were carried out at the same site. One test every 5 m on the track centre and service paths was performed as shown in Fig. 1. Following the German standard (Staatsministerium, 2012), for

each auscultation point, 3 impacts were performed for compaction prior to execution of other 3 impacts for determining the deflection average under the applied load. Using Eqs. (7) and (8) it is possible to calculate the dynamic (E_{vd}) and the static (E_{v2}) moduli from the measured deflections. A total of 24 tests were analysed and the results are shown in Fig. 7. It appears that the test results are stable comparing both tracks along the 30 m experimental site. Moreover, statistical analysis was performed using log-normal distributions (parameters presented in Table 4), showing that the tracks present similar modulus distributions (Fig. 8). In order to correlate these results with those from the PANDA tests, it is assumed that for the on-track LWD test the excited material is only the ballast layer (the 30 cm depth is the auscultation depth of the LWD) and for the on-path tests the excited material is the SBG soil. The mechanical properties of the SBG soil in the lateral path may differ from the SBG under track because their loading history and conditions are not the same. The difference of elastic modulus values from LWD between track (100 MPa) and service path (30 MPa) seems coherent for ballast and silty sand SBG, respectively. A larger data scatter is observed for the on-track (ballast) results but the distributions for both tracks are similar. The standard deviations are also similar for both tracks, and both distributions have the same average value. For the on-path LWD tests, the obtained results show the same distribution for both tracks and lower data scatter as compared to the on-track results. The mean value is lower as the SBG soil has lower stiffness as compared to ballast.

Correlation between the mean values of static modulus (E_{v2}) obtained from the on-track LWD tests and the modulus values estimated from PANDA tests for the ballast layer shows that the values are of the same order of magnitude with less than 25% of difference. In order to facilitate the analysis of the results, a summary of the modulus values obtained from the two prospection methods is shown in Fig. 9. The mean static modulus for the service paths (about 30 MPa) is lower than that for the SBG below the track (77.5 MPa). This could be due to the densification process under the long-time railway traffic loading for the SBG soil below the track. As the ITL

Table 3
Log-Normal distribution parameters of modulus estimated distribution (average and standard deviation) for Ballast, ITL, TL and SBG (PANDA tests performed over tracks 1 and 2).

		Ballast	Interlayer (ITL)	Tran. layer (TL)	Subgrade (SBG)
T1 and T2	μE [MPa]	127	103	95	77.5
	σE [MPa]	78	17	22	53

Table 4
Mean and standard deviations values for dynamic (E_{vd}), elastic modulus (E_{v2}) and CBR obtained from LWD tests for both tracks and service paths.

	E_{vd} [MPa]		E_{v2} [MPa]		CBR	
	μ	σ	μ	σ	μ	σ
Track 1	46	6.1	99.6	14	11	1.2
Track 2	47.3	8.5	103.5	2	11.1	1.9
Path 1	10.6	3.9	21.1	8	3	0.8
Path 2	15.8	4	32.6	8.4	4.5	0.8

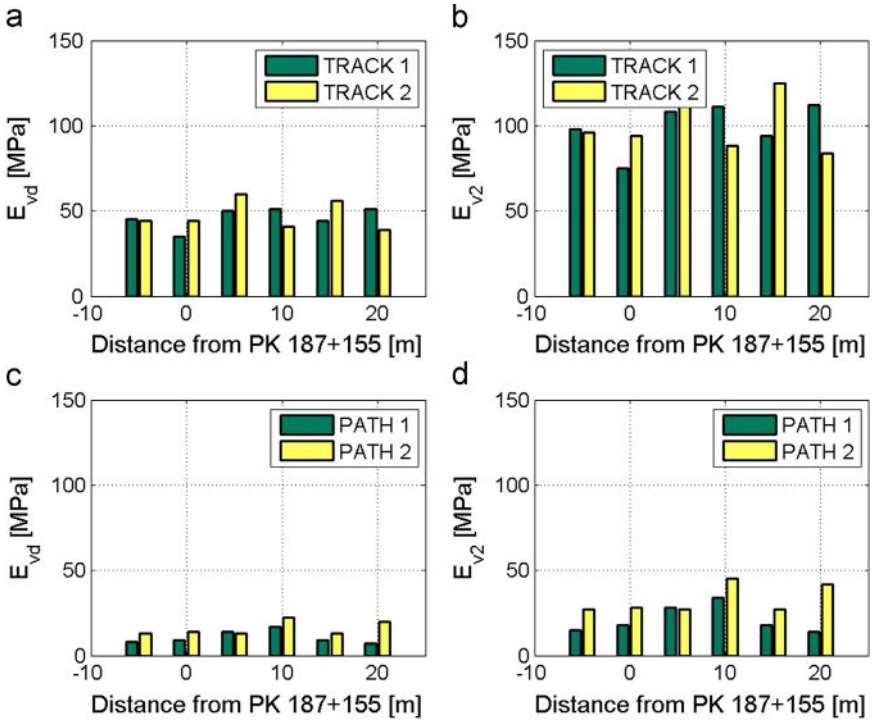

Fig. 7. Results of dynamic (E_{vd}) and elastic modulus (E_{v2}) from LWD tests performed on both tracks (a,b) and service paths (c,d) on the 'Vierzon experimental site'.

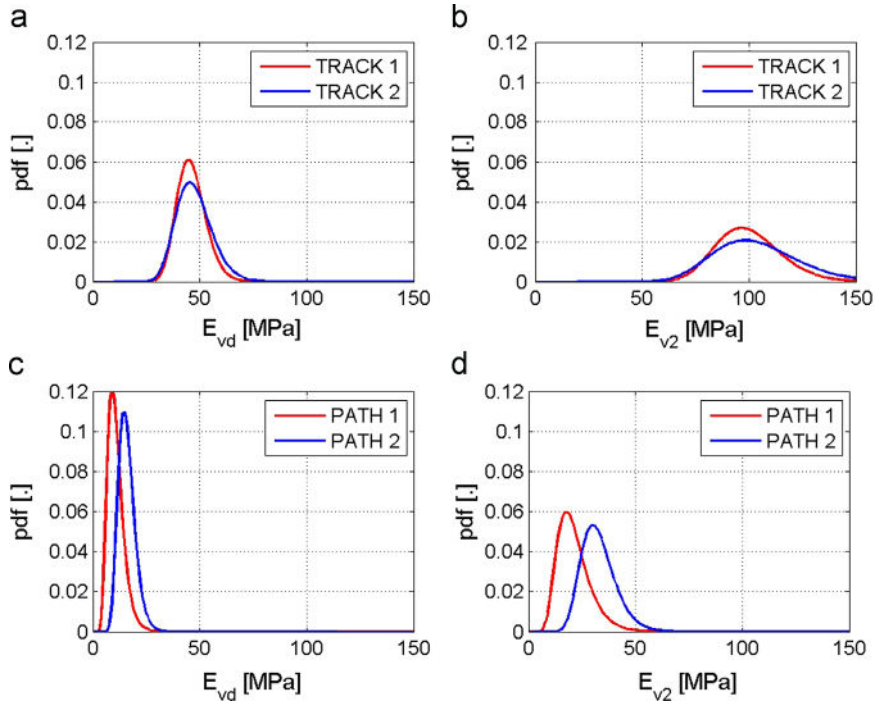

Fig. 8. Log-Normal distribution of dynamic (E_{vd}) and elastic modulus (E_{v2}) from the LWD tests performed on both tracks (a,b) and service paths (c,d).

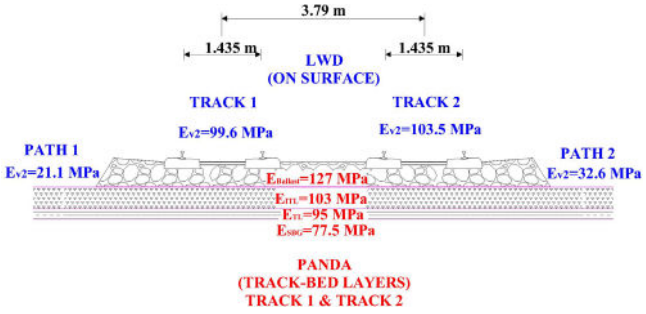

Fig. 9. Summary of modulus estimation from different prospection methods.

and TL soil stiffness values depend on the fractions of ballast and SBG, the moduli of the different materials constituting a track could be inferred from the static modulus obtained from LWD tests on track and lateral path surface: on track the modulus is mainly controlled by the stiffness of ballast layer, while on lateral path surface the modulus of SBG can be obtained. The moduli of ITL and TL must be in between. All the prospection result analyses made allow the definition of a materials' distribution as shown in Fig. 10 for the 'Vierzon experimental site'.

5. Conclusion

A proper investigation is required prior to any renewal or maintenance operations of tracks. In this study, a geotechnical prospection of a representative railway track was performed using geo-endoscopic, PANDA (DCP) and LWD tests.

The Geo-endoscopic tests allow the identification of different materials constituting the platform, their natures and thicknesses. For the prospected site, 4 materials are identified in the track-bed: ballast, interlayer, transition layer and subgrade. A good correlation of thicknesses is obtained between qualitative analysis (geo-endoscopic tests) and quantitative results (PANDA and LWD). The statistical analysis of tip resistance values (PANDA) for different materials and tracks shows a good repeatability of results for both tracks and similar resistance distributions for ballast, ITL and SBG. However, there is more variability for the TL soils in both tracks.

Using empirical formulas, elastic moduli of different materials are estimated: 127 MPa of mean modulus for ballast, 103 MPa for ITL, 96 MPa for TL and 77.5 MPa for SBG. The decreasing modulus over depth appears coherent taking into account the constitution of the track-bed and the nature of each material.

In order to verify the validity of ballast modulus, on-track and on-path LWD tests were carried out at the site. The estimated static modulus on-track was correlated to the modulus estimated from PANDA tests for the ballast layer as the LWD test is limited to the first 30 cm depth. The static modulus values estimated from both tests were found similar. The SBG modulus could be inferred from the LWD tests performed on the lateral service paths, taking into account the lack of densification by the long-time railway traffic loading. As the ITL properties depend strongly on the ballast and SBG fractions, its static modulus is between the values for ballast and SBG.

From the analyses conducted in this study, it appears that the three prospection methods considered are complementary. Empirical formulas can be used to correctly estimate the soil modulus from the tip resistance. Eventually, the LWD test allows the verification of the estimated elastic moduli for

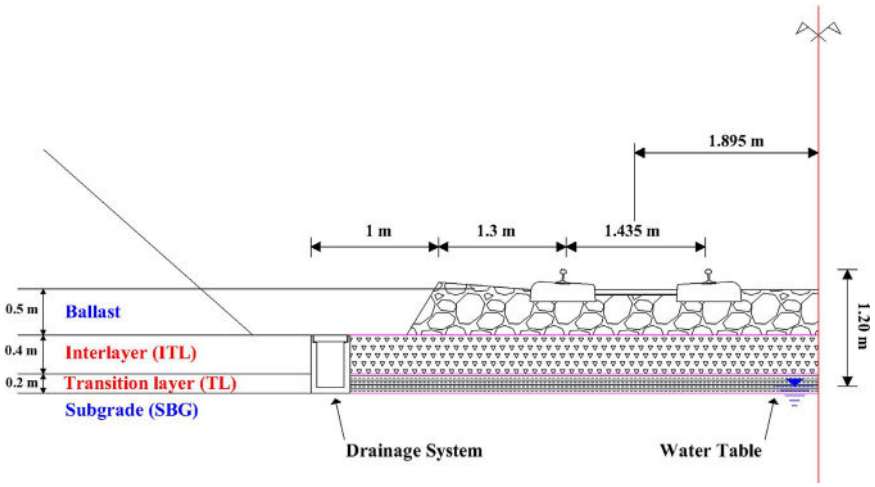

Fig. 10. Profile section of 'Vierzon experimental site' defined after analyses of the prospection tests.

ballast and SBG. The SBG beneath in the track-bed presents a higher modulus than that on paths because of the effect of long-time train loading.

Acknowledgments

This study was conducted within the 'INVICSA' project funded by SNCF-Infrastructure and the ANRT with a CIFRE funding number 2012/1150. The authors are grateful to the SNCF brigade at Vierzon and their work planning manager Ludovic Gaveau for their help in this investigation study on the 'Vierzon experimentation site'.

References

Alves Fernandes, V., Lopez-Caballero, F., Costa d'Aguiar, S., 2014. Probabilistic analysis of numerical simulated railway track global stiffness. Comput. Geotech. 55, 267–276 Elsevier Ltd..

Amini, F., 2003. Potential Applications of Dynamic and Static Cone Penetrometers in MDOT Pavement Design and Construction Final Report.

Araujo, N., 2010. High-Speed Trains on Ballasted Railway Tracks. Dynamic Stress Field Analysis. University of Minho, Portugal.

Benz, M., 2009. Mesures Dynamiques Lors du Battage du Pénétromètre Panda 2 (Doctor of Philosophy Dissertation). University Blaise, France.

Breul, P., 1995. Caractérisation des matériaux de remblai à l'aide de l'endoscopie et de la pénétration dynamique. Clermont Ferrand.

Cassan, M., 1988. Les essais in-situ en mécanique de sols. Tome 1 réalisation et interpretation. (E. Eyrolles, ed.), Paris.

Chai, G., Roslie, N., 1998. The Structural Response and Behavior Prediction of Subgrade Soils using Falling Weight Deflectometer in Pavement Construction. In: Proceedings of the 3rd International Conference on Road and Airfield Pavement Technology.

Chaigneau, L., 2001. Caractérisation des Millieux Granulaires de Surface à l'aide d'un Pénétromètre. Université Blaise Pascal, France.

Chua, K.M., 1988. Determination of CBR and elastic modulus of soils using a portable pavement dynamic cone penetrometer. In: Proceedings of the First Symposium on Penetration Testing ISOPT-1, Orlando, 407.

Connolly, D., Giannopoulos, A., Forde, M.C., 2013. Numerical modelling of ground borne vibrations from high speed rail lines on embankments. Soil Dyn. Earthq. Eng. 46, 13–19 Elsevier.

Cui, Y.-J., Lamas-Lopez, F., Trinh, V.N., Calon, N., D'Aguiar, S.C., Dupla, J.-C., Tang, A.M., Canou, J., Robinet, A., 2014. Investigation of interlayer soil behaviour by field monitoring. Transp. Geotech. 1, 91–105 Elsevier.

Dahlberg, T., 2010. Railway track stiffness variations – consequences and countermeasures. Int. J. Civil Eng. 8 (1), 1–12.

Degrande, G., Schillemans, L., 2001. Free field vibrations during the passage of a thalys high-speed train at variable speed. J. Sound Vib. 247 (1), 131–144.

Duong, T.V., Cui, Y.J., Tang, A.M., Calon, N., Robinet, A., 2014. Assessment of conventional French railway sub-structure: a case study. Bull. Eng. Geol. Environ., 1–12.

Duong, T.-V., Tang, A.-M., Cui, Y., Trinh, V.-N., Dupla, J.-C., Calon, N., Canou, J., Robinet, A., 2013. Effects of fines and water contents on the mechanical behavior of interlayer soil in ancient railway sub-structure. Soils Found. 53 (6), 868–878.

Elaskar, A., 2006. Développement d'une méthode de diagnostic et d'evaluation du potentiel des plates-formes ferroviaires. Mémoire d'ingénieur CUST. Clermont Ferrand.

Fairhurst, C., 1961. Wave mechanics of percussive drilling. Mine Quarry Eng., 169–178.

Haddani, Y., 2005. Caractérisation et Classification des Milieux Granulaires par Geondoscopie. Université Blaise Pascal, France.

Haddani, Y., Saussine, G., Breul, P., Navarrete, M.B., Gourves, R., 2011. Estimation de la portance et de la raideur des plateformes ferroviaires par couplage d'essai Panda et geondoscope. Symposium International GEORAIL.

Hunter, J., Benjumea, B., Harris, J., Miller, R., Pullan, S., Burns, R., Good, R., 2002. Surface and downhole shear wave seismic methods for thick soil site investigations. Soil. Dyn. Earthq. Eng. 22 (9–12), 931–941.

Jacqueline, D., 2014. Caractériser l 'état de serrage du ballast par la propagation d 'ondes. Marne la Vallée.

Livneh, M., Goldberg, Y., 2001. Quality assessment during road formation and foundation construction: Use of falling-weight deflectometer and light drop weight. Transp. Res. Rec. 1755, 69–77.

Lunne, T., Robertson, P.K., Powell, J.J.M., 1997. Cone Penetration Testing in Geotechnical Practice. B. A.-H. Publishers, UK.

Paixão, A., Fortunato, E., Calçada, R., 2014. Transition zones to railway bridges: track measurements and numerical modelling. Eng. Struct. 80, 435–443.

Popescu, R., Deodatis, G., Nobahar, A., 2005. Effects of random heterogeneity of soil properties on bearing capacity. Probab. Eng. Mech. 20 (4), 324–341.

Révol, G., 2005. Mise au point d'une méthode de diagnostic des plates-formes SNCF, mémoire d'ingénieur CUST. Clermont Ferrand.

Rhayma, N., Bressolette, P.H., Breul, P., Fogli, M., Saussine, G., 2011. A probabilistic approach for estimating the behavior of railway tracks. Eng. Struct. 33, 2120–2133 Elsevier.

Shafiee, M., Nassiri, S., Khan, R.H., Bayat, A., 2011. Evaluation of New Technologies for Quality Control/Quality Assurance of Subgrade and Unbound Pavement Layer Moduli.

Staatsministerium, Bayerischen, 2012). Dynamic Plate-Load Testing with the Aid of the Light Drop-Weight Tester. TP BF-StB Part B 8.3.

Steenbergen, M.J.M.M., 2013. Physics of railroad degradation: The role of a varying dynamic stiffness and transition radiation processes. Comput. Struct. 124, 102–111.

Su, L.J., Rujikiatkamjorn, C., Indraratna, B., 2010. An evaluation of fouled ballast in a laboratory model track using ground penetrating radar. Geotech. Test. J. 33 (5).

Su, L., Indraratna, B., Rujikiatkamjorn, C., Christie, D., 2011. Laboratory and field testing study on non-destructive assessment of ballast conditions using ground penetrating radar. In: Proceedings of the 9th World Congress on Railway Reserach, May 22–26.

Sussmann, T.R., Selig, E.T., Hyslip, J.P., 2003. Railway track condition indicators from ground penetrating radar. NDT E Int., 157–167.

Sy, A., Campanella, R.G., 1991. An alternative method of measurement SPT Energy. In: Proceedings of the 2nd International Conference on Recent Advances in Geotechnical Engineering and Soils Dynamics, pp. 499–505.

Tompai, Z., 2008. Conversion between static and dynamic load bearing capacity moduli and introduction of dynamic target values. Period. Polytech. – Civil Eng. 52, 97–102.

Trinh, V.-N., Tang, A., Cui, Y., Dupla, J., Canou, J., Calon, N., Lambert, L., Robinet, A., Schoen, O., 2012. Mechanical characterisation of the fouled ballast in ancient railway track substructure by large-scale triaxial tests. Soils Found. 52, 511–523 Elsevier.

Vorster, D., Gräbe, P., 2013. The use of ground-penetrating radar to develop a track substructure characterisation model. J. S. Afr. Inst. Civil Eng. 55 (3), 69–78.

Woodward, P.K., Kennedy, J., Laghrouche, O., Connolly, D.P., Medero, G., 2014. Study of railway track stiffness modification by polyurethane reinforcement of the ballast. Transp. Geotech. 1, 214–224 Elsevier Ltd..

Zhou, S., 1997. Caractérisation des sols de surface à l'aide du pénétromètre dynamique léger à energie variable type PANDA. Université Blaise Pascal, Clermont-Ferrand.